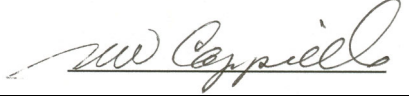|	**Document Release Authorization To IMS**	

Los Alamos National Laboratory

PO Box 1663 MS H816
Los Alamos, NM 87545

This is a milestone document: ☐ YES   ✔ NO

Doc No:	LA-UR-03-7597	Release Date:	10/22/03
Title:	Thermochemistry of Defects and Oxygen Diffusion in Ceria: Preliminary Extension to Plutonia		
Author(s):	Petrica Cristea and Marius Stan, Los Alamos National Laboratory		

Approved for Release

Approved by	Typed Name	Date	Signature
Principal Author:	Petrica Cristea	10/22/03	
LANL Program Manager:	Michael W. Cappiello	10/22/03	

Thermochemistry of Defects and Oxygen Diffusion in Ceria: Preliminary Extension to Plutonia

P. Cristea* and M. Stan**

Los Alamos National Laboratory
PO Box 1663, MS-G755, Los Alamos, NM 87544
*pcristea@lanl.gov, **mastan@lanl.gov

ABSTRACT. Based on a thermochemical model of defects in non-stoichiometric ceria, we calculated the non-stoichiometry of CeO_{2-x}, the electronic, and the ionic conductivities, as functions of temperature and oxygen pressure. We proposed three new models of the oxygen diffusivity, compared them with the available experimental data, and determined the best model that allows for accurate predictions of diffusivity for temperatures in the (900-1400 °C) range and $P_{O2} \in (1 \div 10^{-25}$ atm). A preliminary extension of the defect model to PuO_{2-x} shows that, given appropriate parameters, the model is able to describe the non-stoichiometry and oxygen diffusivity in a reasonable way. Further work is necessary to refine the model. The extension to urania was not possible. Other defect species, such as oxygen interstitials, are required to correctly describe urania.

1. INTRODUCTION

Understanding the thermo-chemistry of nuclear fuel materials is an important part of designing better fuels[1]. Modeling can guide the development and optimization of fuel processing parameters, such as particle size, sintering atmosphere, and temperature regime. The modeling of the kinetics of oxygen diffusion in nonstoichiometric oxides is a critical component of the combined experimental and theoretical effort aimed at improving the knowledge of properties and phenomena in nuclear fuel materials. Bulk diffusion is especially important in optimizing fabrication. Together with the phase stability, it governs the formation of homogenous solid solutions in otherwise heterogeneous powder blends [2]. Diffusivity is the controlling parameter in designing "low" temperature processes to retain volatile constituents while developing a microstructure that will be stable in-pile [3]. The type and defect formation mechanism determines the fuel performance. Kinetic properties of point defects govern radiation tolerance, fission product accommodation, fission gas release and microstructural evolution in-pile. The kinetics of this evolution will impact the stability of the fuel during service. Modeling the defects and the mobility of oxygen in oxide fuels opens a path to the modeling of the more complex phenomena of fission products diffusion.

Ceria is also often used as a surrogate material for studies of thermo-chemical properties of actinide based oxides, such as PuO_2 and UO_2. When heated at high temperatures in a reducing atmosphere, these oxides lose oxygen and become sub-stoichiometric in a similar fashion and form iso-structural compounds [4, 5]. Ceria has a Fm3m fluorite structure, with a lattice parameter a = 5.4113 10^{-10} m. As shown in early studies by Bevan and Kordis [6], ceria has a wide range of non-stoichiometry, determined by temperature and oxygen partial pressure. Recently, Mogensen reviewed the physical and chemical properties of pure and doped ceria [7]. As with most of the non-stoichiometric oxides, the thermo-chemical properties are directly influenced by the type and concentration of point defects [5, 8]. The reduction of CeO_2 by

hydrogen has been studied from room temperature to 1200 °C by several complementary techniques [9-12]. The reduction usually results in a stabilized state with the formal composition $CeO_{1.83}$ but thermal treatments at temperatures higher than 720 °C can reduce the ceria further.

The thermo-chemical properties of plutonia and urania have been investigated to some extent through continuum level methods [13-22]. The focus of this first part of the study is ceria. A more detailed review of plutonia and urania properties will be presented in the following report.

A good model for both self and chemical diffusivity of oxygen in metal oxides (and not only), requires a proper theory describing the nature and the concentration of different oxygen defects, as a function of temperature T, and of the partial pressure of oxygen P_{O_2}. The mass-action law is widely used in the literature to calculate the concentration of lattice defects. Unfortunately, this approach well works only at very low defect concentration. In a highly oxygen defective oxide, the interaction and the exclusion effects considerably affect this simple picture. When evaluating the oxygen partial Gibbs free energy $\Delta G_{O_2}(x,T)$ for highly hypo-stoichiometric oxides, a significant departure from experimental data is observed if the effects arising from interaction and the exclusion are neglected. Also, it should be noted here that, in the case of many metal oxides, the electronic conductivity and the ionic conductivity have never been estimated before over an extended range of non-stoichiometry, by including the effects arising from interaction and exclusion.

The ionic conductivity is sometimes related to the oxygen diffusivity by simply assuming an oxygen vacancy mechanism. If a defect is changing its identity during the exchange with an oxygen ion, this picture is no longer appropriate. If the diffusion is mediated by a vacancy mechanism, the bulk oxygen self-diffusivity is controlled by the doubly charged, or by singly charged oxygen vacancies, only in the low hypo-stoichiometry range. Even in this range, other defects and crossing terms make a significant contribution. In some cases, at high hypo-stoichiometry, the charged oxygen defects are almost non-existent, and the diffusion is mainly controlled by the neutral metal (M) oxygen vacancy V_O complexes $(MV_O)^x$ (Kroger-Vink notation).

While for a restricted non-stoichiometric range some information can be extracted from the available ionic and electronic conductivity measurements, modeling over an extended domain is much more complicated. Our numerical results showed that a good agreement with the available experimental data for oxygen diffusivity is obtained only when the contribution of all defects containing oxygen are taken into consideration. Also, in this case, an excellent agreement between calculated and measured electronic conductivities is obtained.

2.   THERMOCHEMISTRY OF DEFECTS

Usually, the free energy of a defective crystal, G^{dc}, can be written as a sum containing the free energy of the perfect crystal G^{pc}, and a contribution ΔG^d due to the defects:

$$G^{dc} = G^{pc} + \Delta G^d \tag{1}$$

The additional contribution involves the free energy of formation ΔG^f and a configurational part $-T\Delta S^{conf}$, arising from the change in the configurational entropy, ΔS^{conf}.

Following Ling [23], we assume that the free energy of defect formation can be written as a superposition of two terms. One term accounts for short-range interaction ΔG^{SR}, while the second involves the long-range effects (i.e. coulombian interaction) ΔG^{LR}:

$$\Delta G^f = \Delta G^{SR} + \Delta G^{LR} \tag{2}$$

As a result, we can write ΔG^d in the following form:

$$\Delta G^d = \Delta G^{SR} + \Delta G^{LR} - T\Delta S^{conf} \tag{3}$$

The configurational entropy depends on the concentration of various defect species, and it is calculated using the Boltzmann relation:

$$\Delta S^{conf} = k_B T \ln \Omega \tag{4}$$

In (4), Ω is the number of ways of arranging all defects in a lattice with a given symmetry, and k_B is the Boltzmann constant.

For each defect type "i", a virtual chemical potential μ_i is introduced in the usual way:

$$\mu_i = \frac{\partial}{\partial N_i}\left(\Delta G^d\right) \tag{5}$$

where N_i represents the total number of "i" defects in the lattice. The virtual chemical potentials contain a contribution arising from defect formation μ_i^f, and a contribution due to the configurational entropy:

$$\mu_i = \mu_i^f - k_B T \sum_j \Gamma_{i,j} \tag{6}$$

where

$$\mu_i^f = \frac{\partial}{\partial N_i}\left(\Delta G^f\right) \tag{7}$$

and $\Gamma_{i,j} = \frac{\partial}{\partial N_i}\left(\ln \Omega_j\right)$.

The number of configurations Ω_i, for N_i "i" type defects in a lattice already containing all $j \neq i$ defects is calculated as:

$$\Omega_i = \frac{\left[\left(\hat{D} + \Delta\hat{D}\right)_i\right]!}{\left[\left(\hat{D} + \Delta\hat{D} - \hat{N}\right)_i\right]! \left(\hat{N}_i\right)!} \tag{8.1}$$

Using (8.1), the change in the configurational entropy given by eq. (4) can be written as:

$$\Delta S^{conf} = k_B T \sum_i \ln \Omega_i \tag{8.2}$$

The matrices $\hat{D}$ and $\hat{N}$ in eq. (8) are given by:

$$\hat{D} = \begin{pmatrix} D_1 \\ D_2 \\ \cdot \\ \cdot \\ D_n \end{pmatrix} \qquad \hat{N} = \begin{pmatrix} N_1 \\ N_2 \\ \cdot \\ \cdot \\ N_n \end{pmatrix} \tag{9}$$

It should be noted that the effect of exclusion is introduced through the $\Delta\hat{D}$ matrix whose elements are $\Delta D_i = -\left[(\hat{e} -_{dia}\hat{e})\hat{N}\right]_i$, where $e_{i,j} = \left[\sum_k \theta_{k,i}(P,T)\right]_{V_{SR_j}}$ and $(_{dia}e)_{i,j} = \delta_{i,j}e_{i,j}$. The

matrix $\hat{e}$ represents the *exclusion matrix* associated with a given short-range interaction envelope (of volume $V_{SR,j}$) enclosing a given "j" type defect in a given lattice. The pair of indices (i,j) runs over all defect types (n). The elements $\theta_{k,i}$ are the weights for excluding a given configuration "k" for an "i" type defect. Notice that if all $\theta_{k,i}$ are zero, the exclusion effects are discarded, and eq. (8) becomes the classical formula for the number of configurations. Below, we introduce the following matrices:

$$\hat{X} = (N_{cationic})^{-1}\hat{N} \qquad \hat{Y} = (N_{cationic})^{-1}\hat{D} \tag{10}$$

where $N_{cationic}$ is the number of cationic sites in a perfect lattice. The $\hat{D}$ matrix elements are related to the number of excluded configurations for a given defect, and in a first approximation these elements are evaluated by considering a minimal exclusion envelope [23].

By assuming that a total number of *r* reactions are involved in generating the defects, at thermodynamic equilibrium, we can write:

$$\left(\sum_k A_k\mu_k\right)_r = 0 \tag{11}$$

At fixed r, the sum over k in (11) involves all defect types and chemical species (including the perfect sites $M_M^\times$, $O_O^\times$ and O_2). The number of equations, r, equals the number of reactions through the defects are generated, and A_k are the corresponding stoichiometric coefficients for these reactions. Because in the surrounding environment the oxygen behaves like a perfect gas, the oxygen chemical potential is $\mu_{O_2} = RT\ln(P_{O_2})$.

Furthermore, the following constraints have to be taken into account:

i.) Charge neutrality of the defective lattice, as a whole:

$$\sum_i Q_i X_i = 0 \tag{11.1}$$

ii.) Lattice structure conservation (no phase transitions):

$$X_{c,max} - X_c(P,T) = \sum_i X_{i,cationic} \tag{11.2i}$$

$$X_{a,max} - X_a(P,T) = \sum_i X_{i,anionic} \tag{11.2ii}$$

with $X_{c,max}$ the maximum ratio of cationic sites, and $X_{a,max}$ the maximum number of anionic sites. In these conditions, the oxygen deficiency is calculated as:

$$X = X_{a,max} - X_a(P,T) \tag{11.3}$$

In the present study, five types of defects have been incorporated:
- Singly charged (+e) oxygen vacancies $V_O^\bullet$;

4

- Doubly charged (+2e) oxygen vacancies, $V_O^{\bullet\bullet}$;
- Singly charged (+e) metal-vacancy pair, $(MV_O)^{\bullet}$;
- Neutral metal-vacancy pair, $(MV_O)^{x}$;
- Polarons, $M_M^{/}$;

Figure 1 shows the calcium fluorite type structure and some of the defects incorporated in this model.

The Madelung constants needed in calculations were computed using:

$$M_{C,A} = \left\{ M_{(C,A)O} + M_{(C,A)1}\left[1 - \exp\left(-\frac{D}{\tau_{(C,A)1}} \right) \right] + M_{(C,A)2}\left[1 - \exp\left(-\frac{D}{\tau_{(C,A)2}} \right) \right] \right\} \qquad (12)$$

The low indices C and A stand for cationic and for anionic sites, respectively, $M_{(C,A)O,1,2}$, $\tau_{(C,A)1,2}$, D are constants specific to a given fluorite lattice. Notice that M_C is associated with the reference M^{4+} cation, while M_A is associated with the reference host O^{2-} anion. Also, $Q_C = 4q$, $Q_A = -2q$, and we have to regard these charges as the real charges carried by M^{4+} and O^{2-} host ions.

The system of equations (11-12) can be solved self-consistently by using a suitable developed computer code, for different temperatures and partial oxygen pressures.

Electronic And Ionic Conductivities

Assuming a hopping mechanism involving the small polarons, the electronic conductivity can be calculated with the following general relation:

$$\sigma_e = \frac{B}{T^{\gamma}}\left[M_M^{/} \right]\exp\left[-\frac{E_h(x)}{k_B T} \right] \qquad (13)$$

where B is a constant, γ is the ideality constant for hopping, $\left[M_M^{/} \right]$ is the polaron concentration, and $E_h(x)$ is the activation energy for hopping.

The ionic conductivities were evaluated assuming a two-type oxygen vacancy hopping model, involving singly charged vacancies $V_O^{\bullet}$ and doubly charged vacancies $V_O^{\bullet\bullet}$. The total ionic conductivity is given by:

$$\sigma_i = \frac{B_1}{T^{\gamma_1}}\left[V_O^{\bullet} \right]\exp\left[-\frac{E_{h,1}}{k_B T} \right] + \frac{B_2}{T^{\gamma_2}}\left[V_O^{\bullet\bullet} \right]\exp\left[-\frac{E_{h,2}}{k_B T} \right] \qquad (14)$$

Electronic Diffusivity

The electronic diffusivity was calculated using:

$$D_e = \frac{Bk_B}{q^2}\exp\left[-\left(\frac{E_h(x)}{k_B T} \right) \right] \qquad (15)$$

5

3.   OXYGEN SELF AND CHEMICAL DIFFUSIVITIES

Thermodynamic factor $F(x,T)$. The thermodynamic factor $F(x,T)$ is involved in relating the chemical diffusivity to self-diffusivity, and in our models was calculated with

$$F(x,T) = \frac{\Psi(x)}{2RT} \left| \frac{d(\Delta G_{O_2}(x,T))}{dx} \right| \tag{16}$$

where $\Psi(x)$ is a specific function of non-stoichiometry. Here, and in all the relations that follow, we have to keep in mind that the non-stoichiometry x and x_i $(i = V_O^{\bullet}, V_O^{\bullet\bullet}, (MV_O)^{\bullet}, (MV_O)^{\times})$ are all functions $x(P_{O_2}, T)$, $x_i(P_{O_2}, T)$ of partial pressure of oxygen P_{O_2}, and temperature T. These dependencies are complicated, and were calculated with the above thermo-chemical model, by using an original computer program, developed with MathCad. Note that, if during an experiment the partial pressure of oxygen is fixed, these functions depend on temperature only. Conversely, if an experiment is performed at constant temperature, x and x_i are functions on P_{O_2} only. Below, for convenience, we will write simply x, or x_i. By $\Delta G_{O_2}(x,T)$ we understand the oxygen partial Gibbs free energy for a given non-stoichiometric oxide, at a given temperature and given partial oxygen pressure P_{O2}.

Correlation factor, f(P_{O2},T). At a given non-stoichiometry x, we introduced an average correlation factor, $f(x)$, according to:

$$f(x) = \frac{1}{x} \sum_n x_n f(x_n) \tag{17.1}$$

The partial correlation factors $f(x_n)$ were computed using a formula derived by Nakazato and Kitahara [24], and Tahir-Kheli and Elliot [25], [26]. See also [27].

$$f(x_n) = \frac{1}{1 + \dfrac{[1 - (x_n/2)](1 - f_o)}{[1 + (x_n/2)]f_o}} \tag{17.2}$$

Here, $f_o = 0.653$ is the correlation factor for a cubic simple lattice, at very low non-stoichiometry. In this form, *f(x)* is not providing us with much information, except the intuitive result that the diffusion is less correlated at high non-stoichiometry. To get more information, this function was embedded in the (P_{O_2}, T) domain using the mapping $(P_{O_2}, T) \leftrightarrow x(P_{O_2}, T)$. In this way, eq. (17.1) generates the surface $f(P_{O_2}, T)$.

Models of Oxygen Self-Diffusivity and Oxygen Chemical Diffusivity

Average energies Three models have been tested to calculate the oxygen self and chemical diffusivities.

➢ **MODEL 1** introduces an average energy associated with the defective sites as:

$$\langle E_f(x,T) \rangle = -k_B T \ln \frac{x}{2} \tag{18.1}$$

➤ **MODEL 2** introduces an average energy associated with the defective sites as:

$$\langle E_f(x,T) \rangle = k_B T \sum_{n=1}^{4} P_n(x_n, x) \ln \frac{2}{x_n} \tag{18.2}$$

In (18.2), $P_n(x_n, x) = \dfrac{x_n}{x}$ is the relative probability for the n-type defect is present in a lattice.

Self and chemical diffusivities In both models, MODEL 1 and MODEL 2, the self-diffusivity (tracer) is expressed as

$$D_s(x,T) = \frac{a_o^2(T)}{24} f(x) \nu_O(x,T) \tag{19}$$

and the *chemical diffusivity* as

$$D_C(x,T) = \frac{D_s(x,T)}{f(x)} F(x,T) \tag{20}$$

where $a_O(T)$ is the lattice constant at a given temperature, F(x,T) is given by (16), and the correlation factor f(x) by (17.1). The jump frequency $\nu_O(x,T)$ is given by

$$\nu_O(x,T) = \Gamma_o \exp\left(-\frac{E_{av}}{k_B T}\right) \exp\left(\frac{\langle E_{f(1,2)}(x,T) \rangle}{k_B T}\right) \tag{21}$$

In this relation, $\nu_O(x,T)$ is the frequency associated with the jump of an oxygen atom into a defective site, E_{av} is the activation energy for an oxygen jump in MO_{2-x} (assumed to be a constant), Γ_o is a constant. The low-indices in $\langle E_{f(1,2)}(x,T) \rangle$ indicate the model involved in calculation, and $\langle E_{f(1,2)}(x,T) \rangle$ for MODEL 1 and MODEL 2 are calculated with (18.1) and (18.2), respectively.

➤ **MODEL 3** uses following relation for calculating the chemical diffusivity:

$$D_C = D(T) \sum_n C_n x_n^2 \tag{18.3}$$

where:

$$D(T) = D_o \exp\left(-\frac{\langle E \rangle}{k_B T}\right) \tag{18.4}$$

In (18.4) D_o is the Arrhenius pre-exponential diffusivity (considered constant), $\langle E \rangle$ is an average Arrhenius activation energy, C_n are constant coefficients, and *n* runs over all oxygen defect species.

4. RESULTS AND DISCUSSION

4.1   Non-stoichiometric CeO$_{2-x}$

Oxygen deficiency.

As stated above, the defects incorporated in the thermochemical calculations were singly charged (+e) oxygen vacancies $V_O^{\bullet}$, doubly charged (+2e) oxygen vacancies, $V_O^{\bullet\bullet}$, singly charged (+e) metal-vacancy pair, $(CeV_O)^{\bullet}$, neutral metal-vacancy pair, $(MV_O)^{\times}$, and small polarons $Ce_{Ce}^{/}$ (Ce^{3+} ions). Between these defect species, we have considered the same chain of reactions as proposed by Ling [23], with slightly different enthalpies and entropies as parameters (TABLE 1.)

$$O_O^{\times} + 2Ce_{Ce}^{\times} \leftrightarrow \frac{1}{2}O_2 + V_O^{\bullet\bullet} + 2Ce_{Ce}^{/} \tag{19.1}$$

$$V_O^{\bullet} + Ce_{Ce}^{\times} \leftrightarrow V_O^{\bullet\bullet} + Ce_{Ce}^{/} \tag{19.2}$$

$$Ce_{Ce}^{/} + V_O^{\bullet\bullet} \leftrightarrow (CeV_O)^{\bullet} \tag{19.3}$$

$$Ce_{Ce}^{/} + V_O^{\bullet} \leftrightarrow (CeV_O)^{\times} \tag{19.4}$$

TABLE I. The enthalpies and the entropies used the calculations.

Reaction	Enthalpy (eV)	Entropy (eV/K)
19.1	4.93	1.44×10^{-3}
19.2	0.17	-3.1×10^{-4}
19.3	- 0.25	0
19.4	-0.15	6.95×10^{-5}

The lattice constant of CeO$_2$ at room temperature is a$_o$=5.4113 Å [28], and its dependence on the temperature is $a_o(T) = a_o[1 + \alpha(T - 300)]$ with $\alpha =$12.3x10^{-6} K^{-1} [7] (and the references therein). We also included a correction for polarization effects as:

$$\varepsilon_r = \varepsilon_{r,o}(1 - \zeta x) \tag{20}$$

with x the nonstoichiometry in CeO$_{2-x}$, $\zeta = 0.12$, and $\varepsilon_{r,o}$=25 the relative dielectric permitivity of CeO$_2$. The Madelung constants were calculated with eqs. (12), and the parameters are given in TABLE II.

TABLE II. The parameters used in calculation of cationic and anionic Madelung constants.

CATIONIC (C)	ANIONIC (A)
M_{CO} = - 8.325516x10^{-9} (C/m)	M_{AO} = 3.02828x10^{-9} (C/m)
M_{C1} = - 0.42289x10^{-9} (C/m)	M_{A1} = 0.14448x10^{-9} (C/m)
M_{C2} = 5.28338x10^{-9} (C/m)	M_{A2} = 1.10008x10^{-9} (C/m)
τ_{c1} = 6.99332	τ_{a1} = 23.91898
τ_{c2} = 0.72014	τ_{a2} = 2.1184
D = 1000	

The calculated nonstoichiometry at various partial pressures and temperatures are presented in Figure 2, together with a collection of experimental data from [29], [30], [7], [23]. The numerical modeling over an extended range of nonstoichiometry x in CeO_{2-x} confirms that the small polarons Ce'_{Ce}, singly charged vacancies $V_O^{\bullet}$, doubly charged vacancies $V_O^{\bullet\bullet}$, neutral pairs $(CeV_O)^{\times}$, and singly charged pairs $(CeV_O)^{\bullet}$ are the main species to be taken into consideration. In the very low nonstoichiometry region, the small polarons Ce'_{Ce} and doubly charged oxygen vacancies $V_O^{\bullet\bullet}$ are the dominating species. The intermediate region is controlled by $V_O^{\bullet}$, and the deep nonstoichiometry region by the neutral pairs $(CeV_O)^{\times}$. It should be noted that in this region the small polarons and singly charged vacancies make almost the same contribution and this behavior seems not to be influenced by the temperature. While in the very low (x < 0.05) and intermediate (x $\cong$ 0.1) nonstoichiometry region the traditional mass-action theory can still be applied. For the deep nonstoichiometry region (x>0.2) the exclusion effects and the interaction between different species need to be taken into account. Even with the coulombic interaction taken into consideration, the predicted nonstoichiometry lightly exceeds (3-4 %) the experimental values.

Figure 3 shows the calculated oxygen partial Gibbs free energies, as a function of oxygen deficiency and temperature. To make clear the effect of interaction between defects, in one calculation the interaction was neglected. As is clearly seen, while in the low nonstoichiometry range this practically has no influence on the results, in the deep nonstoichiometry region a significant deviation appears.

The relative contribution of different defect species to the oxygen deficiency is of particular importance for the diffusion modeling. This contribution was calculated for different partial oxygen pressures and temperatures. The results in Figure 4. are for 1100 $^{\circ}$C, but the general pattern remains practically unchanged at different temperatures.

Electronic conductivity Following the works of Blumenthal and Panlener [31], Blumenthal and Hofmaier [32], Tuller and Nowick [33], Naik and Tien [34] (see also [7]) it is now accepted that the electronic conductivity involves the hopping of small polarons. The stability of the association between a vacancy and the corresponding Ce^{3+} ions was investigated by atomistic calculations by Conesa [35]. One of these ions was located far from the vacancy ($\cong$ 10 Å away). He observed that, after relaxation, such a singly ionized state is less stable by an amount of 0.47

eV, than the state having both Ce^{3+} ions close to the vacancy. This value is close to the reported 0.4 eV value of the activation energy [33].

To evaluate the electronic conductivity of CeO_{2-x}, we used eq. (13) and a hopping activation energy given by:

$$E_h(x) = E_{ho} + ex \qquad (21)$$

where x is the oxygen deficiency, $E_{ho} = 0.383$ eV, and e = 0.42 eV. In addition, we have considered that the ideality factor is unity $\gamma = 1$, and B = 1.44×10^{-20} SKm^2. A comparison between the calculated results and the reported experimental data [36], [33] is presented in Figure 5.

Ionic conductivity. The ionic conductivity as a function of nonstoichiometry in CeO_{2-x} was calculated with a two-type oxygen vacancy-hopping model, involving singly charged vacancies $V_O^{\bullet}$ and doubly charged vacancies $V_O^{\bullet\bullet}$ (eq.14). The parameters were $B_1 = 1.016 \times 10^{-17}$ SKm^2, $\gamma_1 = 1$, $E_{h1} = 2.2$ eV; $B_2 = 4.49 \times 10^{-19}$ SKm^2, $\gamma_2 = 1$, $E_{h2} = 1.8$ eV. The results are presented in Figure 6. The ionic conductivity in the low nonstoichiometry region is almost entirely due to doubly charged vacancies, while in the high nonstoichiometric ceria, the ionic conductivity is dominated by the singly charged vacancies.

Oxygen diffusivity The suitable function $\Psi(x)$ for CeO_{2-x} is given by $\Psi(x) = (2 - x/2)^{3/2} x^{2/3}$. The thermodynamic factor $F(x,T)$ was calculated with eq. (16), and the results are presented in Figure 7. Using the results from the thermochemical calculations, the correlation factor $f(P_{O2},T)$ was calculated as a function of partial pressure of oxygen for five different temperatures. The results are presented in Figure 8. As expected, in the high nonstoichiometry region, the diffusion of oxygen is less correlated. Note that the results of thermochemical calculations and (17.1) allow for an in depth investigation of contributions due to different defect species to the correlated diffusion. Figure 9 shows the average energies as defined by (18.1) – MODEL 1, and (18.2) – MODEL 2, as a function of oxygen deficiency.

To calculate the self and the chemical diffusivities, the following parameters have been used:

For MODEL 1 and MODEL 2: $E_{av} = 1.69$ (eV), $\Gamma_o = 8.82 \cdot 10^{15} \, s^{-1}$;

For MODEL 3: $D_O = 1.1 \times 10^8 \frac{k_B}{q}$ cm^2/s, $\langle E_a \rangle = 2.1$ eV. The coefficients C_n are given in TABLE III.

TABLE III. The coefficients C_n used in MODEL 3.

$C_1(V_O^{\bullet\bullet})$	$C_2(V_O^{\bullet})$	$C_3[(CeVO)^{\bullet}]$	$C_4[(CeVO)^{\times}]$
95	1.3	5.3	0.45

With these values, the self and the chemical oxygen diffusivities have been calculated at different oxygen pressures (stoichiometry) and different temperatures. An example is shown in Figure 10. Additionally, a comparison with the experimental data reported by Kamiya [37] is included in Figure 11. We can see that results calculated within MODEL 2 are in a remarkable good agreement with the experimental data. MODEL 1 slightly overestimates the diffusivities in the high temperature range. Figure 12 presents a comparison between the reported experimental

diffusivities for various Ce-M-O solutions, and the results calculated with MODEL 1, and MODEL 2.

4.2. Nonstoichiometric PuO$_{2-x}$

Oxygen deficiency. We have used the same model to evaluate the oxygen deficiency in PuO$_{2-x}$, as a function of temperature and oxygen partial pressure. The enthalpies and the entropies for the chain (19.1)-(19.4) are given in TABLE IV. The calculated oxygen deficiencies at different temperatures and partial oxygen pressures were compared with the experimental data in Figure 13. We have a reasonable good agreement, but we have to realize that more experimental data and theoretical studies are needed before deciding about the nature of the defect species and about their formation energies in this material.

TABLE IV. The enthalpies, and the entropies used in calculations.

Enthalpy (eV)	Entropy (eV/K)
4.8	0.55x10^{-3}
0.2	-2.5x10^{-4}
- 0.1	0
-0.3	0

Oxygen diffusivity. From a least square fit of log(D) as function of 1/T Deaton et al [38] found a chemical diffusivity close to $D = 1.19 \cdot 10^{-3} \exp(42200/RT)$ [cm^2/s]. The Arrhenius energy for diffusion of oxygen in PuO$_2$ is then close to 42.2 kcal/mole. This is equivalent to 1.83 eV/particle. It should be noted that this Arrhenius energy compare favorably with 29.7 kcal/mole for UO$_2$ [39], and 56.0 kcal/mole for ZrO$_2$ [40], all of which are oxides with fluorite structure.

The results calculated with MODEL 3 were compared with the data above, in the nearly stoichiometric PuO$_2$, using eq. (18.3), and an average Arrhenius energy $\langle E \rangle$=1.83 eV. The same coefficients C_n as for nonstoichiometric ceria were used. Because we are in the nearly stoichiometric range, we need C_1, and C_2 only. The results are presented in Figure 14, together with the experimental data from [38].

4.3. Nonstoichiometric UO$_{2\pm x}$

Very little data is available about hypostoichiometric urania. Because even at very low nonstoichiometry, UO$_{2\pm x}$ defective lattice includes a significant amount of oxygen interstitials, a direct extension of the previous calculations to this material is not possible in this stage. The results of a more elaborate model including the effect of oxygen interstitials will be presented in the next report.

CONCLUSIONS

1. Numerical modeling over an extended range of nonstoichiometry x in CeO_{2-x} confirms that the small polarons Ce'_{Ce}, singly charged vacancies $V_O^{\bullet}$, doubly charged vacancies $V_O^{\bullet\bullet}$, neutral pairs $(CeV_O)^{x}$, and singly charged pairs $(CeV_O)^{\bullet}$ are the main defect species in this material.

2. In the very low nonstoichiometry region, the small polarons Ce'_{Ce} and doubly charged oxygen vacancies $V_O^{\bullet\bullet}$ are the dominating species. The intermediate region is controlled by $V_O^{\bullet}$, and the deep nonstoichiometry region by the neutral pairs $(CeV_O)^{x}$. It should be noted that in this region the small polarons and singly charged vacancies make almost the same contribution and this behavior seems not be influenced by the temperature.

3. While in the very low (x < 0.05) and intermediate (x $\cong$ 0.1) nonstoichiometry region the traditional mass-action theory can still be applied, for the deep nonstoichiometry region (x>0.2) the exclusion effects and the interaction between different species need to be taken into account.

4. Even with the coulombic interaction taken into consideration, the predicted nonstoichiometry lightly exceeds (3-4 %) the experimental values.

5. The thermochemical calculations were extended to PuO_{2-x} and the calculated oxygen deficiencies are in reasonable good agreement with the previous published experimental data.

6. The electronic, and the ionic conductivities of CeO_{2-x}, were calculated as functions of temperature and oxygen pressure over an extended range of oxygen deficiency. The calculated results are in a good agreement with reported experimental data.

7. We proposed three new models of the oxygen diffusivity, compared them with the available experimental data, and determined the best model (MODEL 2) that allows for accurate predictions of diffusivity for temperatures in the (900-1400 °C) range and $P_{O2} \in$ ($1 \div 10^{-25}$ atm).

8. The termodynamic factors and the correlation effects were studied as a function of composition and temperature.

9. A preliminary extension of the defect model to PuO_{2-x} shows that, given appropriate parameters, the model is able to describe the non-stoichiometry and oxygen diffusivity in a reasonable way. It should be noted that more experimental data and theoretical studies are needed before deciding about the nature of the defect species and about their formation energies in this material.

10. Because even at very low nonstoichiometry, $UO_{2\pm x}$ defective lattice includes a significant amount of oxygen interstitials, a direct extension of the previous calculations to this material is not possible in this stage.
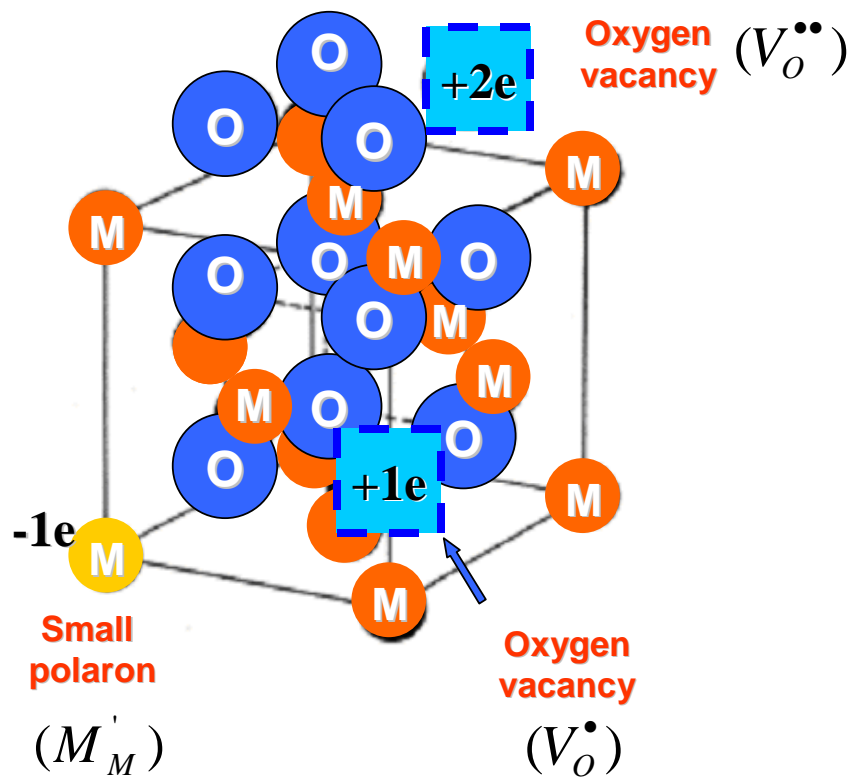
Figure 1. The calcium fluorite type structure and some of the defects incorporated in this work. $V_O^{\bullet}$ - singly charged oxygen vacancy; $V_O^{\bullet\bullet}$ - doubly charged oxygen vacancy; $M_M^{/}$ - small polaron.
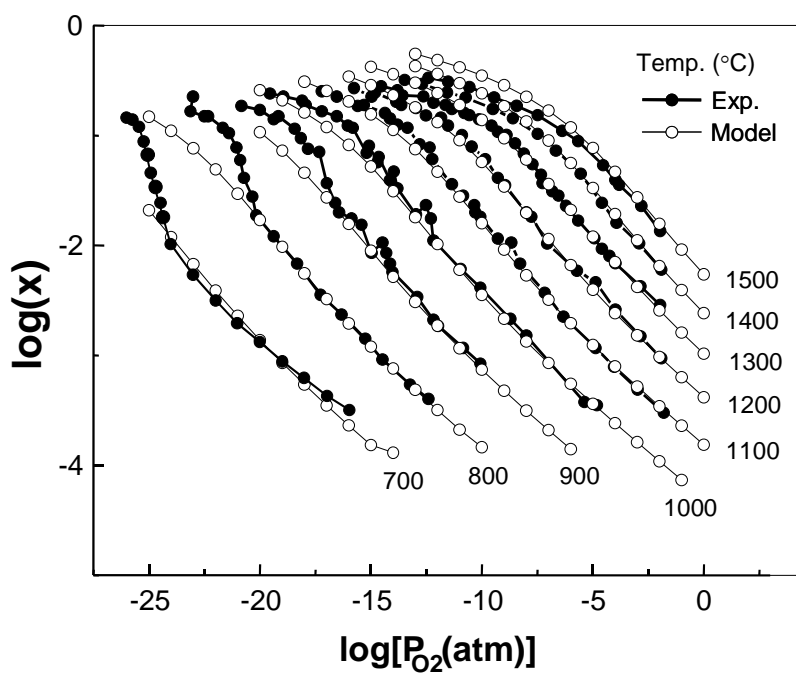
Figure 2. Oxygen nonstoichiometry x in CeO$_{2-x}$, as a function of oxygen partial pressure, and temperature. The experimental data are compiled from [29]. The experimental data at 700 ^{o}C are from [41]
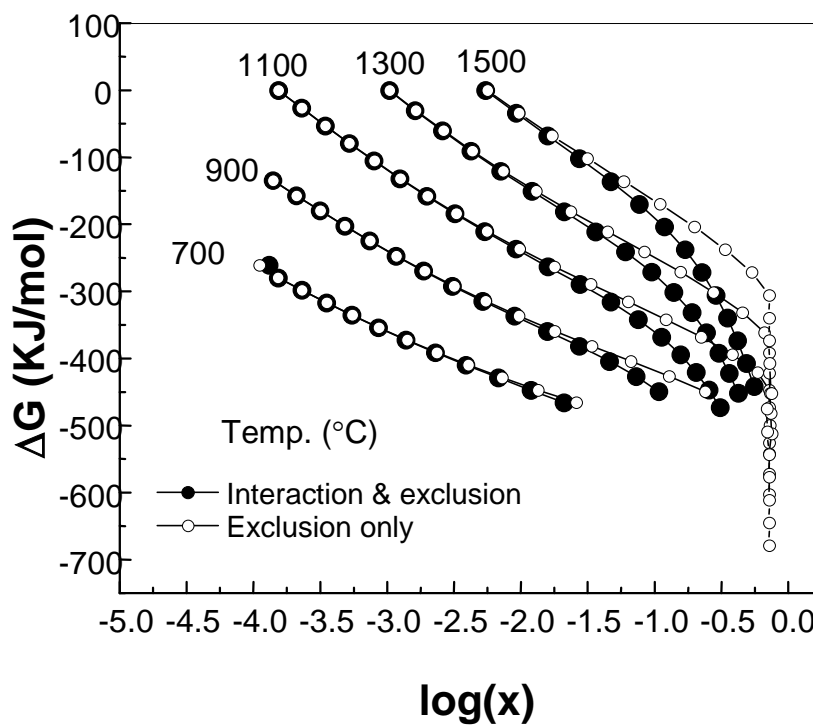

Figure 3. The oxygen partial Gibbs free energy in CeO$_{2-x}$ as a function of non-stoichiometry.
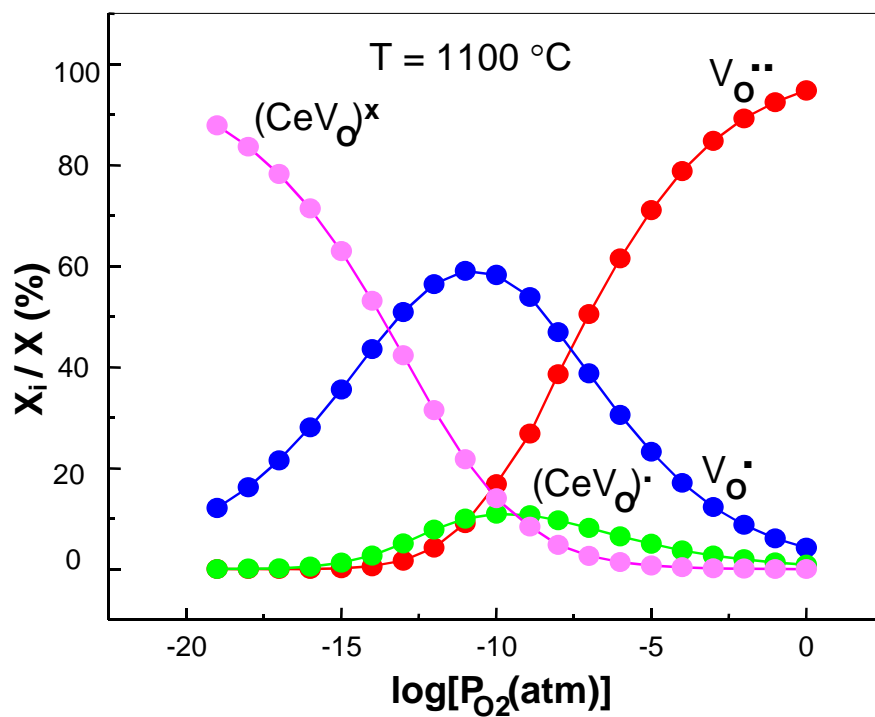
Figure 4. Calculated relative contribution of defect species to the nonstoichiometry of CeO_{2-x}.
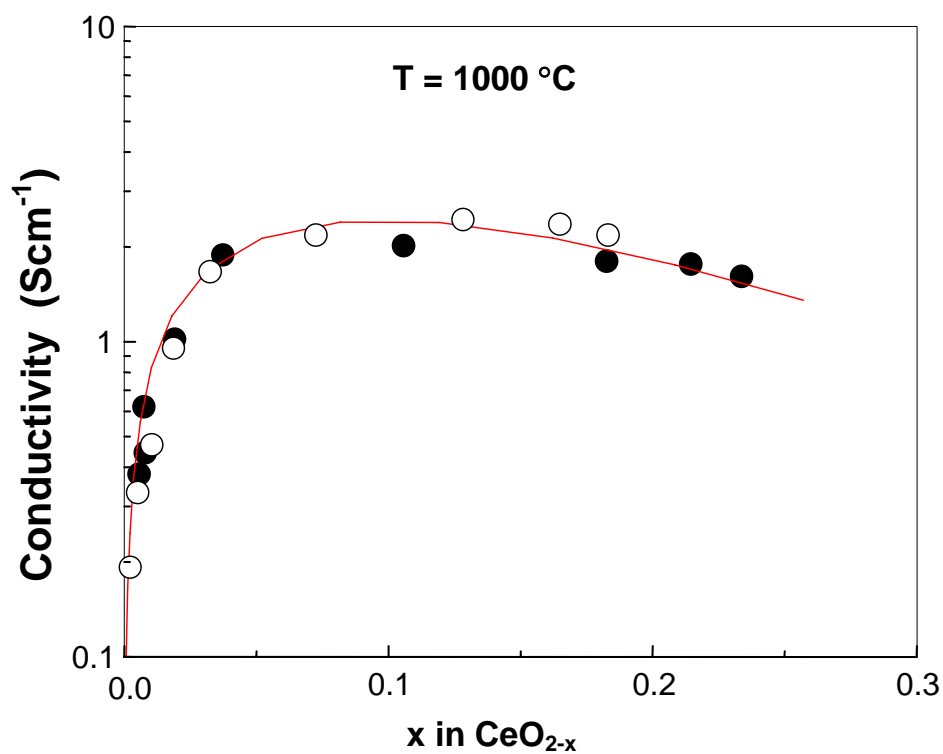
Figure 5. Electronic conductivity of CeO_{2-x} as a function of nonstoichiometry
Red line – calculated with eq. (13). Circles [36], [7]; black points [33], [7].
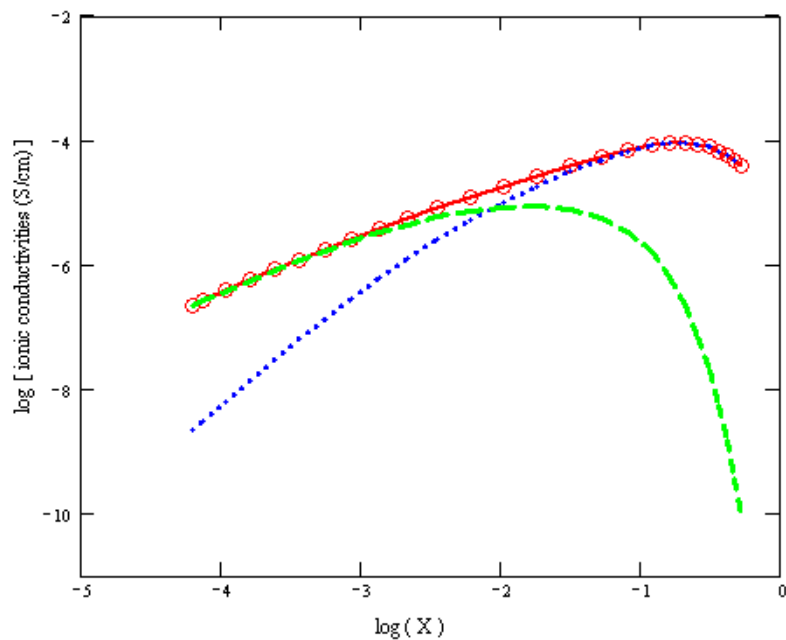
Figure 6. Ionic conductivities in CeO$_{2-x}$, as a function of oxygen deficiency (T=1000 ^{o}C), calculated with eq. 14. Red line – total ionic conductivity; blue line - singly charged vacancies contribution; green line – doubly charged vacancies contribution.
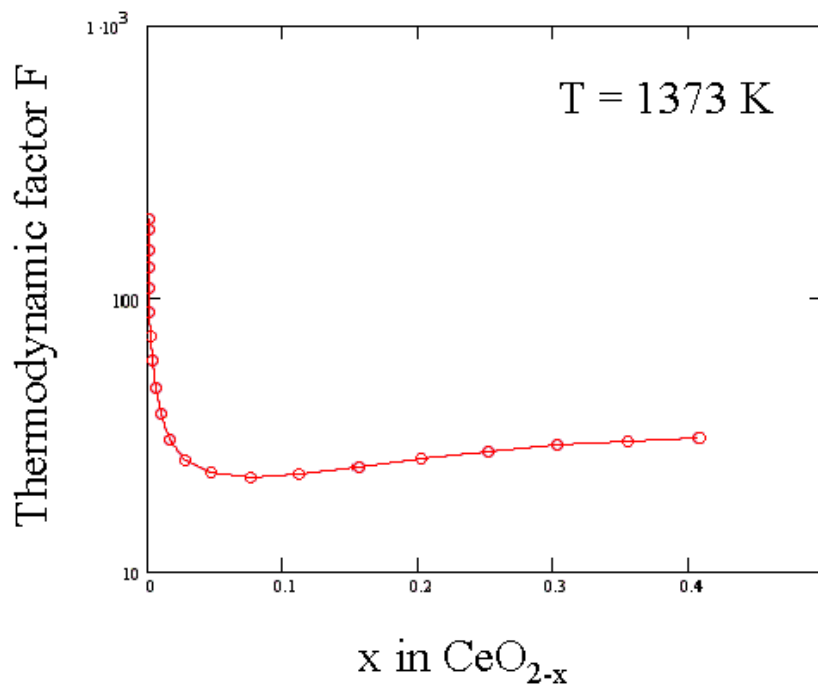
Figure 7. The thermodynamic factor as a function of nonstoichiometry x in CeO$_{2-x}$.
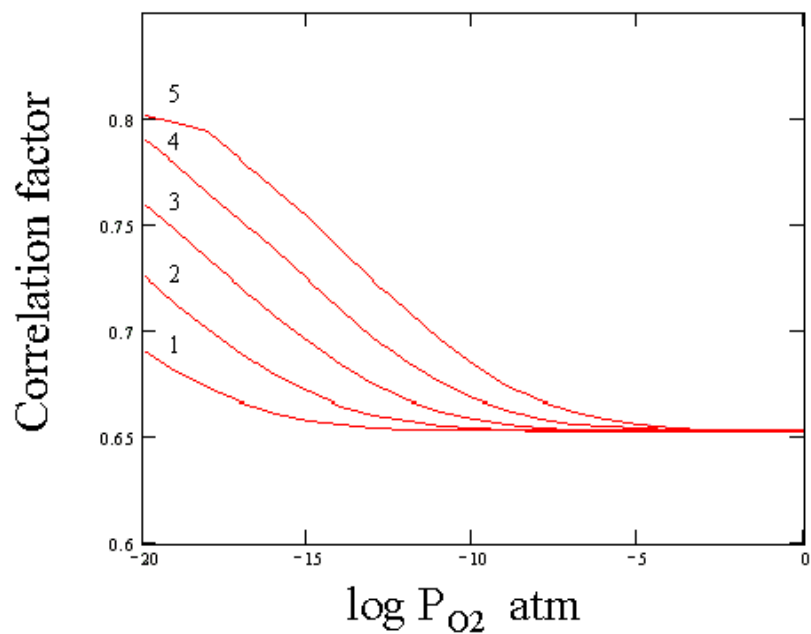
Figure 8. The correlation factor for CeO$_{2-x}$, as a function of partial pressure of oxygen, P$_{O2}$. The parameter is the temperature. (1) 1273 K; (2) 1373 K; (3) 1473 K; (4) 1573 K; (5) 1673 K.
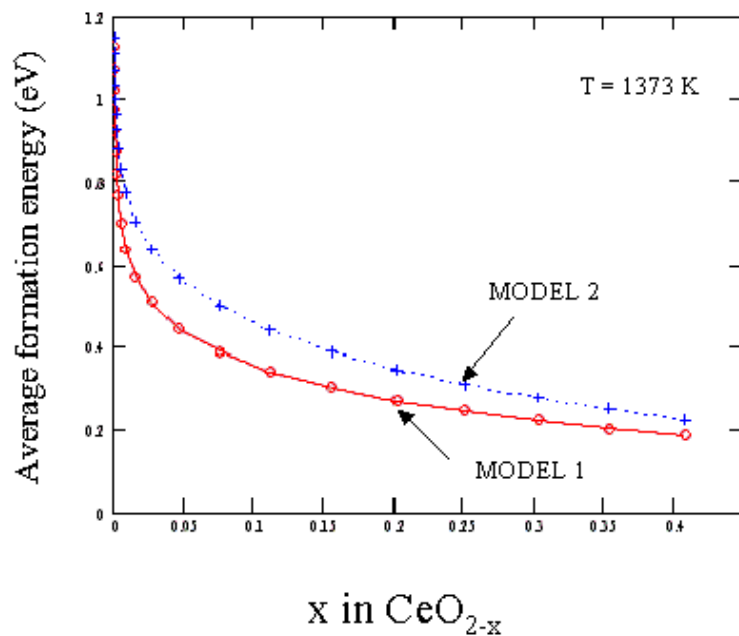
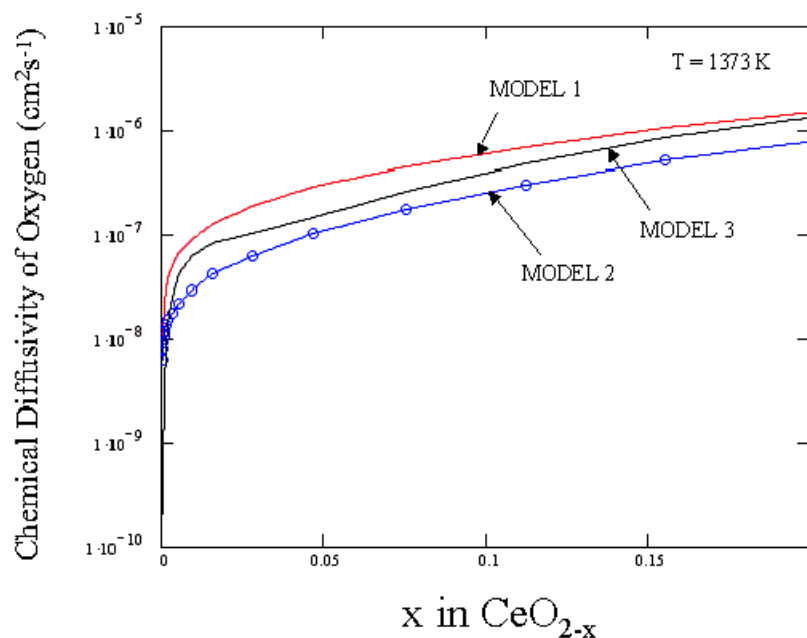Figure 9. Average energies for defective sites, as a function of nonstoichiometry x in CeO$_{2-x}$ (T=1373 K).

Figure 10. Comparison between the chemical diffusivities of oxygen in CeO$_{2-x}$, calculated with the three models, as a function of nonstoichiometry; red line, MODEL 1; blue line MODEL 2; open-circles connected by a black line MODEL 3.
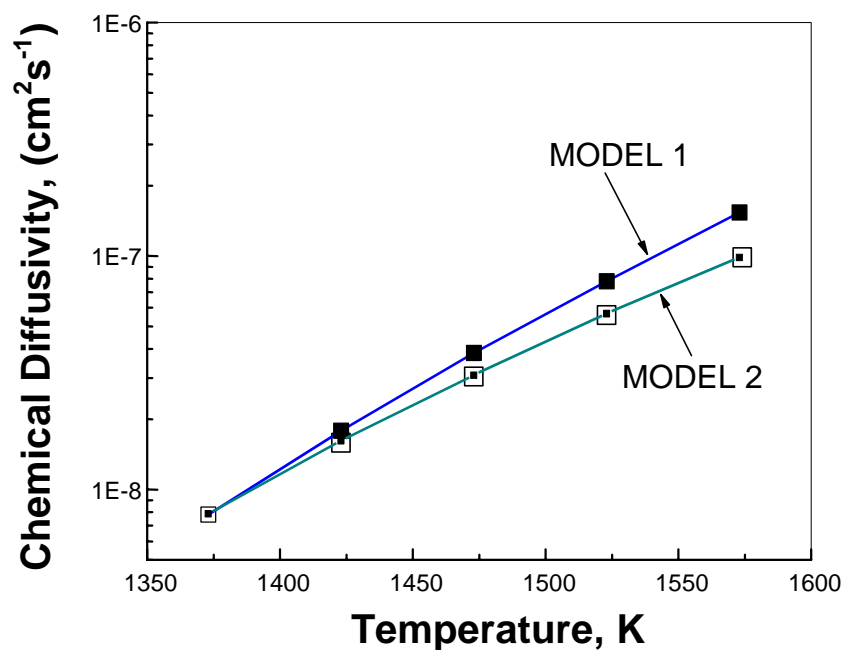

Figure 11. Comparison between the calculated results (MODEL 1 and MODEL 2), and the experimental results reported by Kamiya et *al.*. Blue line – MODEL 1; cyan line –MODEL 2; red squares – Experimental data [37], represented by $D = 3.16\exp(-2.343q/k_BT)$ cm^2/s.
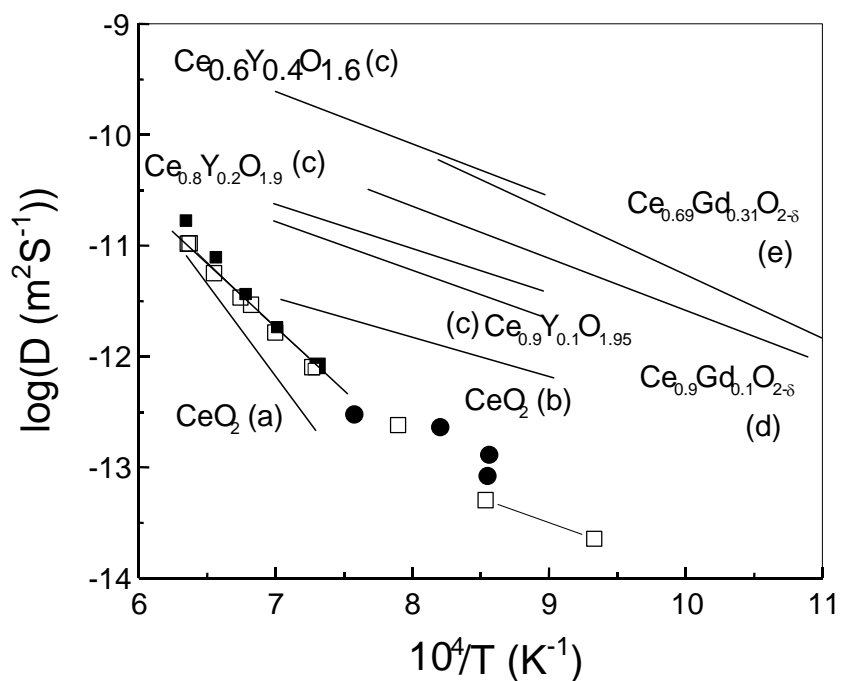
Figure 12. Temperature dependence of oxygen diffusion coefficient in CeO$_2$.
Filled squares – MODEL 1; Empty squares MODEL 2; ● and □ [37]; (a) CeO$_2$ [42], (b) CeO$_2$ [43]; (c) Y-doped CeO$_2$ [43]; (d) Gd-doped CeO$_2$ [44]; (e) Gd-doped CeO$_2$ [45].

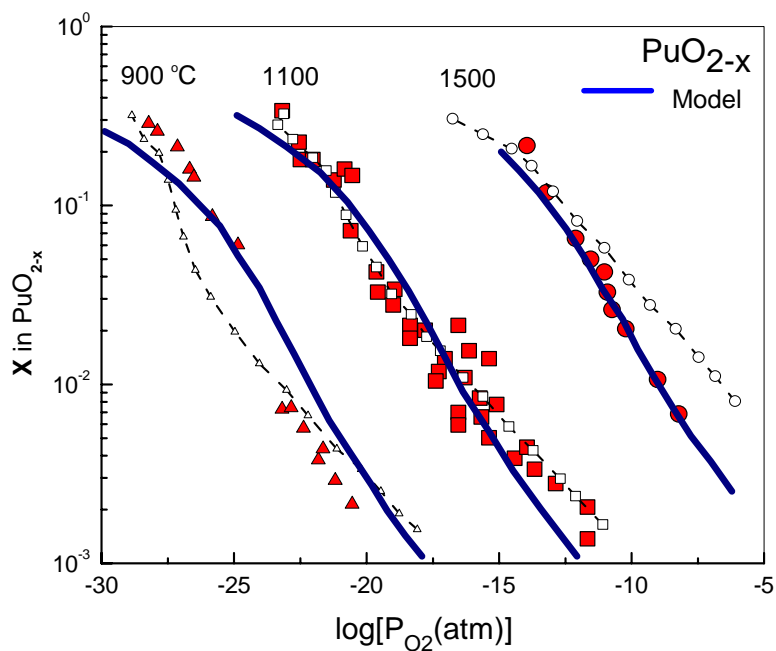Figure 13. Oxygen deficiency of PuO2-x, as a function of oxygen partial pressure and temperature. Open triangles, circles, and squares from Nakamura [5], Red triangles, circles, and squares are compiled from experimental data reported in [46-50]
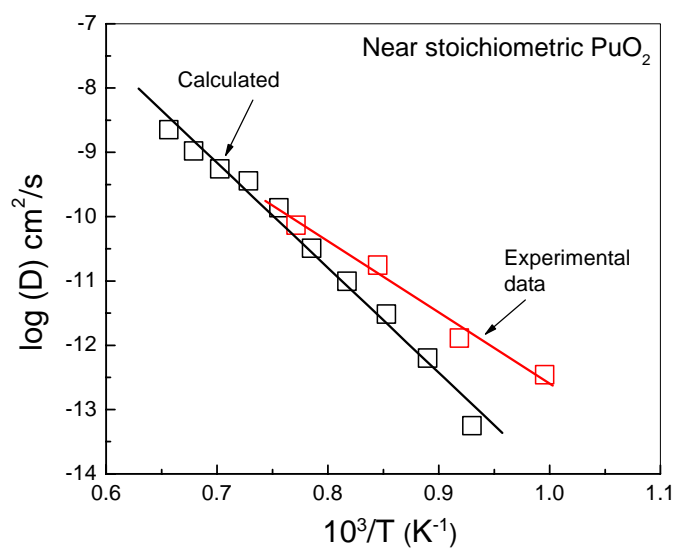
Figure 14. The dependence of oxygen diffusivity on temperature in nearly stoichiometric PuO$_2$.
Black squares - MODEL 3; red squares experimental data [38].

REFERENCES

[1] T. Ogawa, M. Akabori, F. Kobayashi, and R. G. Haire, J. Nucl. Mater., **247** (1997) 215-221.

[2] M. Beaivy, J. Nucl. Mater., **188** (1992) 232-238.

[3] E. K. Storms, J. Nucl. Mater., **132** (1985) 231-243.

[4] M. Stan, T. J. Armstrong, D. P. Butt, T. C. Wallace, Y. S. Park, C. L. Haertling, T. Hartmann, and R. J. Hanrahan, J. Amer. Ceram. Soc., **85** (2002) 2811-2816.

[5] A. Nakamura, J. Nucl. Mater., **201** (1993) 17-26.

[6] D. J. M. Bevan and J. Kordis, J. Inorg. Nucl. Chem., **26** (1964) 1509-1523.

[7] M. Mogensen, N. M. Sammes, and G. A. Tompsett, Solid State Ionics, **129** (2000) 63-94.

[8] R. Dieckmann, J. Phys. Chem. Solids, **59** (1998) 507-525.

[9] V. Perrichon, A. Laachir, S. Abouarnadasse, O. Touret, and G. Blanchard, Applied Catalysis a-General, **129** (1995) 69-82.

[10] V. Perrichon, A. Laachir, G. Bergeret, R. Frety, L. Tournayan, and O. Touret, Journal of the Chemical Society-Faraday Transactions, **90** (1994) 773-781.

[11] A. Laachir, V. Perrichon, A. Badri, J. Lamotte, E. Catherine, J. C. Lavalley, J. Elfallah, L. Hilaire, F. Lenormand, E. Quemere, G. N. Sauvion, and O. Touret, Journal of the Chemical Society-Faraday Transactions, **87** (1991) 1601-1609.

[12] C. Lamonier, G. Wrobel, and J. P. Bonnelle, J. Mater. Chem., **4** (1994) 1927-1928.

[13] G. Berggren and R. S. Forsyth, *Some Studies of the High Temperature Behavior of PuO2 and PuO2-Uo2 Mixtures*, in A. E. Kay and M. B. Waldron, eds., *Plutonium 1965*, Chapman and Hall, London, 1965, pp. 828-834.

[14] T. M. Besmann, J. Nucl. Mater., **144** (1987) 141-150.

[15] T. M. Besmann and T. B. Lindemer, J. Am. Ceram. Soc., **66** (1983) 782-785.

[16] T. M. Besmann and T. B. Lindemer, J. Nucl. Mater., **130** (1985) 489-504.

[17] T. M. Besmann and T. B. Lindemer, J. Nucl. Mater. (1986).

[18] T. B. Lindemer, (1986).

[19] T. B. Lindemer, Calphad, **13** (1989) 109-113.

[20] T. B. Lindemer and T. M. Besmann, J. Nucl. Mater., **130** (1985) 473-488.

[21] T. D. Chikalla and C. E. McNeilly, Am. Ceram. Soc. Bull., **48** (1969) 460-&.

[22] G. R. Chilton and I. A. Kirkham, Plutonium and Other Actinides, (1976) 171-183.

[23] S. Ling, Phys. Rev. B, **49** (1994) 864-880.

[24] K. Nakazato and K. Kitahara, Prog. Theor. Phys., **64** (1980) 2261-2264.

[25] R. A. Tahir-Kheli, Phys. Rev. B, **28** (1983) 3049-3056.

[26] R. A. Tahir-Kheli and R. J. Elliott, Phys. Rev. B, **27** (1983) 844-857.

[27] A. R. Allnatt and A. B. Lidiard, *Atomic Transport in Solids*, Cambridge University Press, Cambridge, 1993.

[28] J. R. Sims and R. N. Blumenthal, High Temp. S., **8** (1976) 99-110.

[29] H. TULLER and A. NOWICK, J. Electrochem. Soc., **126** (1979) 209-217.

[30] R. PANLENER, R. BLUMENTHAL, and J. GARNIER, J. Phys. Chem. Solids, **36** (1975) 1213-1222.

[31] R. N. Blumenthal and R. J. Panlener, J. Phys. Chem. Solids, **31** (1970) 1190.

[32] R. N. Blumenthal and R. K. Sharma, J. Solid State Chem., **13** (1975) 360-364.

[33] H. L. Tuller and A. S. Nowick, J. Phys. Chem. Solids, **38** (1977) 859-867.

[34]   I. K. Naik and T. Y. Tien, J. Phys. Chem. Solids, **39** (1978) 311-315.

[35]   J. C. Conesa, Surf. Sci., **339** (1995) 337-352.

[36]   R. N. Blumenthal, P. W. Lee, and R. J. Panlener, J. Electrochem. Soc., **118** (1971) 123.

[37]   M. Kamiya, E. Shimada, Y. Ikuma, M. Komatsu, and H. Haneda, J. Electrochem. Soc., **147** (2000) 1222-1227.

[38]   R. L. Deaton and C. J. Wiedenheft, J. Inorg. Nucl. Chem., **35** (1973) 649-650.

[39]   A. B. Auskern and J. Belle, J. Chem. Phys., **28** (1958) 171-172.

[40]   A. Madeyski and W. W. Smeltzer, Mater. Res. Bull., **3** (1968) 369.

[41]   R. J. Panlener, R. N. Blumenthal, and J. E. Garnier, J. Phys. Chem. Solids, **36** (1975) 1213-1222.

[42]   M. Kamiya, E. Shimada, and Y. Ikuma, J. Ceram. Soc. Jpn., **106** (1998) 1023-1026.

[43]   J. M. Floyd, Indian J. Technol., **11** (1973) 589-594.

[44]   P. S. Manning, J. D. Sirman, and J. A. Kilner, Solid State Ionics, **93** (1996) 125-132.

[45]   E. RuizTrejo, J. D. Sirman, Y. M. Baikov, and J. A. Kilner, Solid State Ionics, **115** (1998) 565-569.

[46]   T. L. Markin and M. H. Rand, *Thermodynamics; Proceedings of the Symposium on Thermodynamics with Emphasis on Nuclear Materials and Atomic Transport in Solids, Vienna, Austria, 1965*, International Atomic Energy Agency, Vienna, Vol. I, 1966, pp. 145.

[47]   G. C. Swanson, *Los Alamos National Laboratory Report (LA-6063-T)*, 1975.

[48]   L. M. Atlas and G. J. Schlehman, *Thermodynamics; Proceedings of the Symposium on Thermodynamics with Emphasis on Nuclear Materials and Atomic Transport in Solids, Vienna, Austria, 1965*, International Atomic Energy Agency, Vienna, Vol. II, 1966, pp. 407.

[49]   O. T. Sorensen, *in Plutonium 1975 and other actinides : Proceedings of the Conference in Baden Baden, September 10-13, 1975 / 5th International Conference on Plutonium and Other Actinides, 1975*, North-Holland Pub. Co., Amsterdam, 1976, p. 123.

[50]   R. E. Woodley, J. Nucl. Mater., **96** (1981) 5-14.